ELSEVIER

Journal of Molecular Structure: THEOCHEM 762 (2006) 123–132

THEO CHEM

www.elsevier.com/locate/theochem

Bonding in metal–carbonyls: A comparison with experiment and calculations on adsorbed CO

M. Nyberg [a], A. Föhlisch [b], L. Triguero [a], A. Bassan [a], A. Nilsson [a,c], L.G.M. Pettersson [a,*]

[a] *FYSIKUM, AlbaNova University Center, Stockholm University, S-106 91 Stockholm, Sweden*
[b] *Institut für Experimentalphysik, Universität Hamburg, Luruper Chaussee 149, D-22761 Hamburg, Germany*
[c] *Stanford Synchrotron Radiation Laboratory, 2575 Sand Hill Road, Menlo Park, CA 94025, USA*

Received 5 October 2005; received in revised form 5 October 2005; accepted 5 October 2005
Available online 4 January 2006

Abstract

The general aspects of CO bonding in carbonyls and on metal surfaces are discussed in terms of a molecular orbital description, based on calculations and direct experimental measurements. In particular, the excellent agreement between experiment and theory for CO adsorbed on Ni(100) is the starting point to derive in the same theoretical approach the orbital-based electronic structure of the carbonyls $Ni(CO)_4$, $Fe(CO)_5$, $Cr(CO)_6$ and CO coordinated to the heme group. A frontier orbital interaction scheme involving only the $2\pi^*$ and the 5σ orbitals is shown to be inadequate for the description of the electronic structure; all orbitals change due to the interaction. Instead, we demonstrate how the formation of an allylic configuration in the π-system, involving both the 1π and $2\pi^*$ orbitals, gives a more complete description of the π electronic structure. The rearrangement of the σ orbitals involves mainly mixing of occupied CO and metal orbitals resulting in Pauli repulsion. The latter is minimized by polarization of charge away from the CO–Me bond. The bonding picture for CO in organometallic systems is very similar to the surface adsorption case; the main idea of repulsive σ and bonding π interactions seems generally valid when CO interacts with metals.

Keywords: Metal–carbonyls; Adsorbed CO; Metal

1. Introduction

The interaction between CO and a metal is one of the most well-studied examples of chemical bonding, both from a theoretical and an experimental viewpoint (for recent reviews of this vast field see e.g. [1] and the historical overview given in [2]). In particular, the comparison of carbonyls and CO adsorbed to metal surfaces has turned out to be fruitful in the development and testing of conceptual models of adsorption and organometallic bonding. In the original papers by Dewar [3] and Chatt and Duncanson [4] treating bonding in unsaturated π-systems, as well as in the important paper by Blyholder [5] with application to adsorption problems, the analysis of the orbital structure was made in terms of atomic orbitals on each center, while later work has mostly used an approach with unperturbed molecular orbitals on each interacting fragment. The common textbook description of the bonding in terms of a σ-donation and π^*-backdonation is often illustrated with the simple drawing of the interaction as between the empty π^* orbital with the appropriate d-orbital on the metal as in a frontier–orbital description. It is clear that this is an oversimplified picture and already the earliest papers [3–5] showed that also the 1π-orbital must be involved in the description of bonding in the π-system. However, for the σ-system it is usually assumed that the unperturbed molecular orbitals provide a good starting point for a description of the molecular orbitals of the complex. New experimental techniques in combination with theoretical studies show, however, that this is not correct: there are large changes in the distribution of all the molecular orbitals and a better description of the interaction is in terms of a balance between π-bonding and σ-repulsion [6–9].

The bonding of molecules, such as CO, N_2, ethene and ethyne, with unsaturated π-systems, to a metal is of fundamental importance. In heterogeneous catalysis the molecule binds to the metal atoms in the surface of the catalyst, while in homogeneous catalysis the interaction is with a metal that is already coordinated by other ligands. Due to the importance of these reactions in fundamental chemistry and also to the conceptual simplicity of the traditional picture of the bonding, the Dewar–Chatt–Duncanson (DCD) model [3,4] is

* Corresponding author. Tel.: +46 8 5537 8712; fax: +46 8 5537 8442.
E-mail address: lgm@physto.se (L.G.M. Pettersson).

0166-1280/$ - see front matter © 2005 Elsevier B.V. All rights reserved.
doi:10.1016/j.theochem.2005.10.022

probably one of the most well-known bonding schemes in chemistry. However, the details of the resulting molecular orbital structure have been difficult to investigate experimentally other than indirectly; e.g. ultraviolet photoelectron spectroscopy (UPS) measures the binding energies of the valence electrons and the overall character of the level while infrared spectroscopy (IR) measures the change in the internal CO bonding due to the interaction with the metal. Since no direct experimental measurements of the atomic composition of the different molecular orbitals has been available, it is probably fair to say that the specific orbitals obtained from theoretical calculations have not been given high relevance; the analysis has usually been performed in an average sense, i.e. in terms of resulting total π or σ-populations according to some particular scheme to decompose the density into atomic contributions or as density difference plots based on the total density. The contributions to the energetics in the interaction have been analyzed according to many different schemes to subdivide the relaxation of the density (or molecular orbitals) to form the bonded system from the separated molecules [1]. These types of energy decomposition schemes will always contain some measure of arbitrariness and their applicability depends on their usefulness to reproduce, analyze and predict trends; also here a direct experimental measurement of the orbital polarization effects, atomically resolved, can help to distinguish between energy contributions e.g. due to bonding or to minimization of repulsion.

In order to experimentally study in detail the character of the occupied molecular orbitals (MO) of an adsorption complex one needs a technique that is both atom-specific and capable of resolving the symmetry of the different MO's, e.g. separate σ and π character. In X-ray Emission Spectroscopy (XES) one excites a core electron, e.g. C 1s or O 1s of CO, to the lowest available empty level and detects the photons emitted when one electron from the occupied valence levels subsequently decays to fill the core hole; the energy and polarization of the emitted photon gives information on the energy and character of the specific occupied valence orbitals around the atom with the core-hole [10]. Since the excitation energies of core-levels are strongly element-specific there is no difficulty to separate the elements in the adsorbate and select on which type of atom the core hole should be created; for instance, ionization from C 1s and O 1s in c(2×2)CO/Ni(100) requires 285.8 ± 0.1 and 531.4 ± 0.2 eV, respectively [11]. The binding energy of the core levels is furthermore sensitive to the chemical environment, a fact that is used in e.g. X-ray Photoelectron Spectroscopy (XPS) to characterize oxidation and charge states. This chemical shift can, within XES, be used to separate also atoms of the same type within a molecule by carefully tuning the energy of the synchrotron beam; specific examples include separation of the individual atomic contributions to the MO's of N_2 chemisorbed vertically on the Ni(100) metal surface [7,12] (the nitrogen closest to the surface has its 1s-level shifted to 1.2 eV higher binding energy) and individual spectra from all the (heavy) atoms of glycine on the Cu(110) surface [13].

XES has many of the properties of an experimental atomic population decomposition and as such it is ideally suited for a theoretical analysis [10]. Since the transition involves decay into a core-level, only valence orbitals that have some contribution at that particular site can generate a signal. Since furthermore, for the systems to be discussed in the following, only 1s core orbitals will be used, the XES will only give direct experimental information on the 2p character in each orbital in the spatial region of the 1s orbital. For a full characterization of the atomic contributions in each orbital this must then be combined with theoretical calculations that give information also on the s and d character in the MO's. By combining experiment and theory in this manner, a very detailed and reliable picture of the individual molecular orbitals, based on direct measurement, can be obtained also for complex chemisorption systems. The bonding scheme deduced in this way for chemisorbed N_2 and CO is based on π-bonding and σ-repulsion. The 2p orbitals of the adsorbate form bonding, non-bonding and completely anti-bonding π-symmetry combinations with the d-orbitals of the substrate in an allylic configuration [7,8,14]; since only the bonding and non-bonding (lone-pair state) are strongly occupied this results in net bonding in the π-system. The σ-system has no low-lying counterpart to the π^* orbital and is thus much less polarizable. As a result the doubly occupied adsorbate 4σ and 5σ orbitals rearrange to minimize the Pauli repulsion against mainly the substrate d_σ level. This is accompanied by metal rehybridization and polarization to further reduce the repulsion [7–10].

The experimental technique, when applied to chemisorption complexes, is presently limited to well-ordered adsorbates and high coverages, but the resulting picture of the bonding in terms of an essentially repulsive σ-interaction and the formation of three new orbitals (bonding, non-bonding and totally anti-bonding) from the individual *atomic* 2p and 3d orbitals in the π-symmetry is a general one and applies also to e.g. CO bonding to organometallic complexes. In the following we will first calibrate our theoretical approach by comparison with CO adsorbed on Ni(100) for which experimental data exist [8,9]. Having thus validated our approach we will present our results for some organometallic complexes, i.e. $Ni(CO)_4$, $Fe(CO)_5$, $Cr(CO)_6$ and CO bonding to the hemegroup of hemoglobin and show that the proposed picture of the interaction and bonding remains valid also for these systems. We choose to present our results in the form of computed XES spectra in order to compare the results for the carbonyls directly with the experimental data on chemisorbed CO. The dependence of the resulting orbital shapes on the position of the 3d levels will be discussed through a computational comparison between gas phase TiCO and NiCO.

2. Theoretical methods

The calculations have been done at the gradient-corrected Density Functional Theory (DFT) level using the program StoBe-deMon [15] with the exchange functional by Perdew and Wang, and the correlation functional by Perdew [16]. The orbital basis sets used were of triple-zeta + polarization quality for the non-metal atoms for which the orbitals were analyzed through their XES spectra, while for the metals a

standard double-zeta basis was used for the s and p orbitals and triple-zeta (including a diffuse d) for the 3d. The calculations on chemisorbed CO used a Ni_{13} all-electron cluster model of the metal substrate for the on-top and hollow species, while a Ni_{14} cluster was used for the bridge site in order to exploit the symmetry in the two different cases.

The calculation of X-ray emission spectra was also done using the StoBe-deMon implementation for X-ray spectroscopy studies [10,17]. The transition energies on a binding energy scale were taken as the ground state orbital energies with only an overall shift of all orbital energies to make the calculated HOMO orbital energy the zero-level. The XES intensities were calculated using the ground state orbitals [18], where explicit dipole transition moment integrals were calculated for transitions between the carbon or oxygen 1s orbital and the valence orbitals; this procedure has proven very reliable in a large number of applications [10,19].

The structures of both the coordinated heme group with CO and the metallocarbonyls were furthermore fully optimized using energy gradients prior to calculating theoretical spectra. Interaction energies were analyzed in terms of the Constrained Space Orbital Variation (CSOV) scheme [20]; the partitioning of the orbital space will be described in the text. Symmetry-resolved charge density differences between the separated and combined systems are used to illustrate the flow of electrons between symmetries as a result of the bond formation.

3. Results

3.1. CO Chemisorbed on Ni(100)

The experimental data for CO adsorption in different sites, i.e. in on-top, bridge and four-fold hollow positions of the Ni(100) surface, have been reported in ref. [9]; these are reproduced in Fig. 1 together with our computed spectra symmetry-resolved in π and σ-components. In on-top adsorption CO binds with the carbon to a single metal atom, in the bridge site to two and finally in the hollow position it interacts directly with five metal atoms. The possibilities for a bonding overlap increase with the coordination, but so does the repulsion in the σ-system. The net result is very similar chemisorption energies for the different sites combined with very different vibrational frequency red-shifts and large effects on the electronic structure as observed in XES and also obtained from the calculations.

In order to facilitate the discussion, we will consistently use the local σ or π character of the CO molecule to label the orbitals; for the bonded systems, where the orbital changes are large, we will indicate the dominating contribution as e.g. $\tilde{\sigma}$ to show that, in this example, the gas phase σ-orbital has been strongly modified through the interaction. The calculations reproduce the experimental trends quite well, with the increasing polarization of the 1π orbital towards the carbon with increased coordination, while the 5σ polarizes away from the substrate. In the π-system we observe the formation of a bonding 1π orbital at the highest binding energy, followed by a non-bonding oxygen lone-pair state with no intensity on the

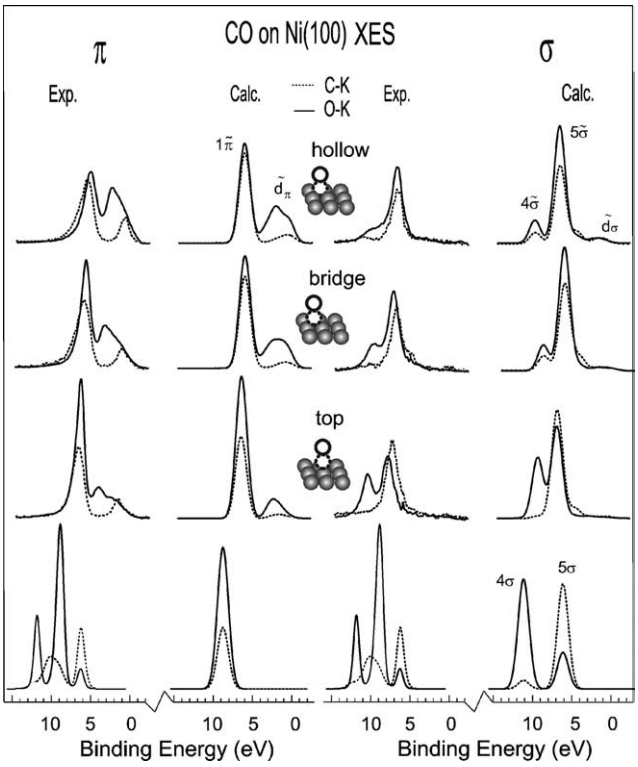

Fig. 1. Experimental and computed XE spectra for CO in gas phase and adsorbed at different sites of the Ni(100) surface[9]. The XE spectra for the adsorbate systems are referred to the Fermi level while the gas phase spectra are referred to the respective gas phase core-level binding energies.

carbon. Close to the Fermi level we find a third state with contributions from both carbon and oxygen corresponding to the totally anti-bonding orbital; the electronic structure in the π-symmetry thus corresponds to an allylic configuration. The 5σ orbital polarizes towards the outer (oxygen) atom and the 4σ towards the inner (carbon) atom (mainly C2s character). The relative strength of the 4σ- and 5σ-states in the oxygen XE spectrum is a measure of the degree of polarization upon adsorption. In the free CO molecule the intensity of the 4σ is ≈5 times larger than the 5σ in the oxygen spectrum (the experimental spectrum is here complicated by strong configuration-interaction effects as well as by the fact that the symmetries cannot be separated due to the lack of order in the gas phase). On Ni, this ratio changes dramatically and the 4 $\tilde{\sigma}$ is even weaker than the 5$\tilde{\sigma}$. The degree of polarization increases with increasing Ni coordination. In the π-system we observe the dominant 1π state in both the carbon and oxygen XES spectra. Towards lower binding energy, new states are observed, which differ in the oxygen and carbon spectra. We denote these spectral features as the $\tilde{d}_\pi$ band. At the bottom of this band (higher binding energy), intensity is only observed in the oxygen spectrum. This state is the characteristic oxygen lone-pair state of π-symmetry. At the top of the band, close to the Fermi-level, intensity is present in both the carbon and oxygen XES data. The 1π forms a bonding combination with the metal d-states, maximizing overlap through internal polarization towards the carbon end of the molecule. At the same time a characteristic lone-pair state at the outer atom is

formed with large Ni d-character. Both the amount of 1π polarization and adsorbate character in the lone pair state increase with increasing Ni coordination. We note that the 1π orbital for CO in the hollow site has the same contribution on both atoms, which is rather different compared with the free molecule.

Both the π-bonding and the σ-repulsion increase with increasing Ni coordination in such a way that the resulting adsorption energy is rather similar between on-top and bridge sites and only slightly less favorable for hollow sites. The gain in increasing π bonding is thus lost due to the increased σ repulsion.

From these results we can derive a model of the surface chemical bond which is different from the traditional picture of the DCD or Blyholder model in that it involves strong modifications of all molecular orbitals and where the resulting binding energy is obtained from a balance between repulsion in the σ system and bonding based on the π orbitals. Instead of bonding through σ donation the main effect from the σ system is thus a repulsive interaction.

This clearly demonstrates the energy balance between the two different orbital systems and has been proposed as the origin of the difficulties at the DFT level to describe reliably the site-preference of adsorbed CO on Pt(111) [21]: since the rather small binding energy differences result from the balance between attractive and repulsive contributions, which vary strongly between sites, this is a real challenge to theoretical treatment. The question is now whether this bonding picture can be transferred to metal carbonyls and to CO coordinated to hemoglobin.

3.2. CO in metallorganic compounds

Having calibrated our theoretical approach against the XE spectra of adsorbates, where such experiments could be performed, let us now turn to metal coordination chemistry in order to investigate how general the obtained bonding model is. We will focus particularly on the molecular orbital structure and energy contributions for a series of metal carbonyls and finally for CO coordinated to the heme group of hemoglobin.

We like to present the molecular orbital structure in an atom-specific picture in direct comparison with experiment and will, therefore, simulate theoretical XE spectra projected on the C and O atomic sites in the CO group. Fig. 2 shows computed XE spectra for free CO, CO in the on-top site of the Ni surface, $Ni(CO)_4$, $Fe(CO)_5$, $Cr(CO)_6$ and CO coordinated to the heme group. The molecular orbital structure in the different metal carbonyls will be governed by the respective symmetry point group where the ligand interactions split the molecular orbitals in a number of different states. In order to facilitate a comparison with the adsorbate and between different carbonyls we project locally the π- and the σ contributions within one CO ligand.

Let us first compare CO adsorbed on the Ni surface and a CO in $Ni(CO)_4$. We can see in Fig. 2 that the π spectra closely resemble each other. This is further illustrated in orbital contour plots of some of the most relevant orbitals, shown in

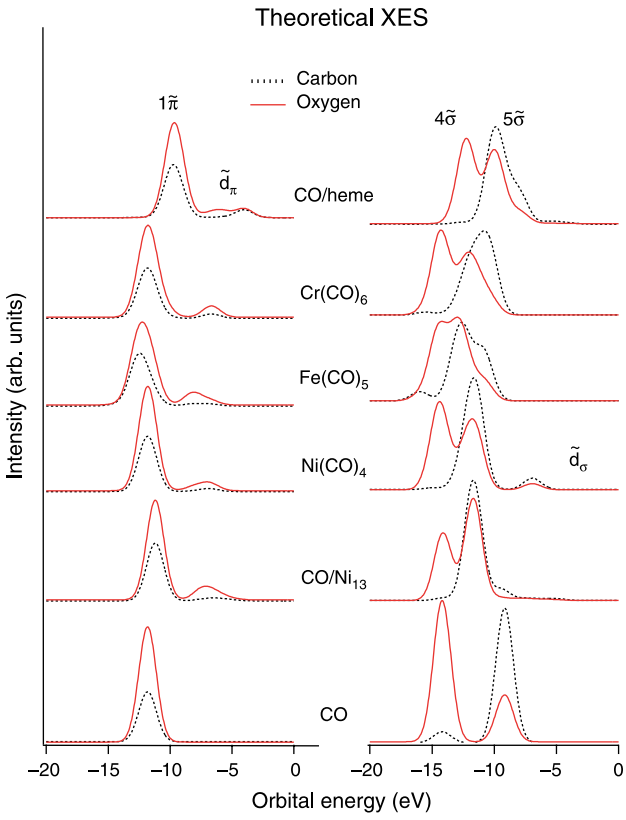

Fig. 2. Computed XES spectra of CO in the gas phase, adsorbed on-top on Ni surface, in metal carbonyls and coordinated to the heme group.

Fig. 3. As seen in the calculated XE-spectra, the 1π polarizes towards the carbon atom in both the adsorption and metal coordination cases. The metal d_π contribution is found to be higher for adsorption on Ni in the surface than in $Ni(CO)_4$, as evidenced by the larger intensity in the lone-pair state in the former case. As seen from the contour plots, Fig. 3, the 1 $\tilde{\pi}$ has the same phase between the O, C and metal centers, constituting a node-less bonding orbital between all atomic centers in line with the allylic configuration.

In the two middle panels of Fig. 3 orbital plots from two different energy regions within the $\tilde{d}_\pi$-band are shown. We have labeled the orbital representing the high binding-energy region at the 'bottom of the band' as the $\tilde{d}_\pi$-b and the orbital close to the Fermi-level or HOMO at the 'top of the band' as $\tilde{d}_\pi$-t; for $Ni(CO)_4$ this corresponds to the e and t_2 levels, respectively. The orbital plots of the $\tilde{d}_\pi$-b and $\tilde{d}_\pi - t$ are characterized by a nodal plane between the oxygen atom and the metal atoms. It is also evident that these orbitals are mainly of metal d-character. These orbitals correspond nicely to the lone pair non-bonding orbital in the allylic configuration described in the previous section.

In the top panel of Fig. 3 we show the 2π* and 2$\tilde{\pi}$* orbitals which are unoccupied and therefore not seen in the simulated XE spectra.

From this comparison we can directly note the same local allylic orbital structure for adsorbed CO and CO in $Ni(CO)_4$. The difference between the two systems is mainly that the d_π contribution in the 1 $\tilde{\pi}$ and the CO character in the $\tilde{d}_\pi$-band is

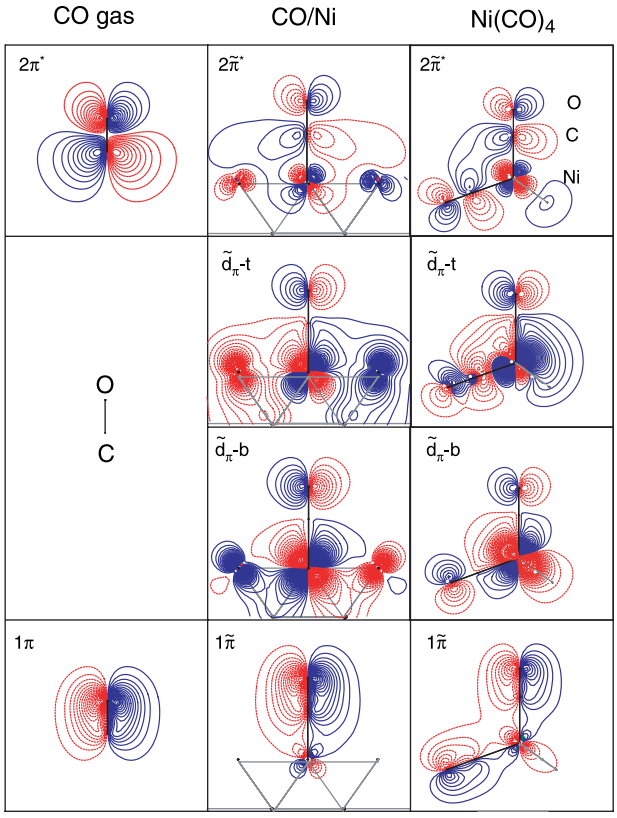

Fig. 3. Contour-plots of π-orbitals for CO in the gas phase, adsorbed in on top position on the Ni_{13} cluster and in $Ni(CO)_4$. Atom positions indicated in upper right panel. Line spacing in panels; top: 0.02, center: 0.01, bottom: 0.02. Solid and dashed lines symbolize a change of sign.

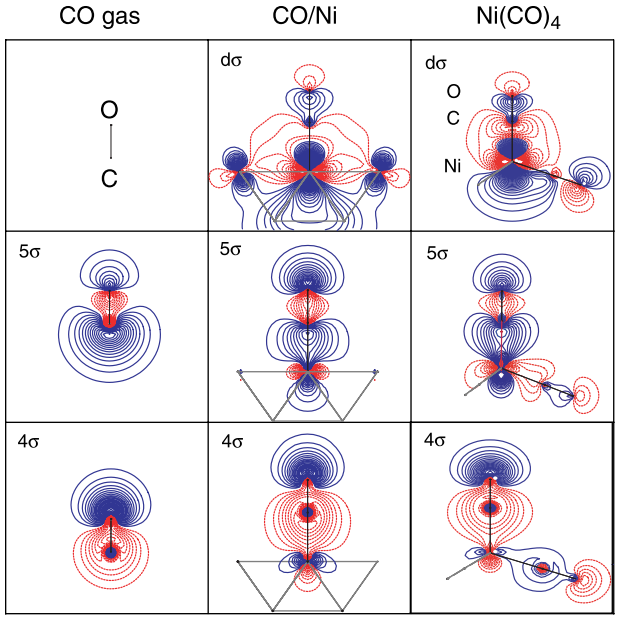

Fig. 4. Contour-plots of σ-orbitals for CO in the gas phase, adsorbed in on top position on the Ni_{13} cluster and in $Ni(CO)_4$. Line spacing in panels; top: 0.01, center and bottom: 0.02. Solid and dashed lines symbolize a change of sign.

smaller for $Ni(CO)_4$ as compared with the adsorbate. This indicates a slightly lower overall π interaction in the carbonyl compound, which can be attributed to a larger number of CO molecules per Ni atom.

If we now turn to the σ system shown in Fig. 2 we can see a similar orbital polarization for CO in $Ni(CO)_4$ as for surface-adsorbed CO. This is further illustrated in the σ orbital contour plots shown in Fig. 4. In both cases we note a polarization of the $5\tilde{\sigma}$ orbital towards the oxygen. The 4σ orbital looses 2p character both on oxygen and on carbon upon metal coordination. This is because the 4σ gains mainly C(2s) character after the adsorption which is not seen in the simulated XE spectra since only atomic p-angular momentum is seen in this spectroscopy. The metal contribution in both the 5 $\tilde{\sigma}$ and 4 $\tilde{\sigma}$ is in a bonding phase between CO and Ni. The polarization effects are larger for the adsorbate than in the case of $Ni(CO)_4$ which is easily seen in the XE spectra. This indicates a smaller σ interaction for the metal carbonyl.

We have now established that the local orbital structure is rather similar for $Ni(CO)_4$ and adsorbed CO on Ni in on-top position. In order to examine the energetical effects associated with π and σ contributions we have performed constrained space orbital variation (CSOV) calculations [20]. The results are summarized in Table 1 together with values taken from ref. [22]. In this partitioning scheme, the interaction energy between the two fragments is decomposed into its constituents by stepwise relaxing part of the orbital space. We have done this for three systems, namely CO chemisorbed on Ni, and for the case of a CO molecule interacting with $Ni(CO)_3$ and $Cr(CO)_5$ fragments to form $Ni(CO)_4$ and $Cr(CO)_6$, respectively. This is similar to the first bond dissociation energy (FBDE) of CO in the different cases, but without inclusion of the energetical effect of geometrical relaxation of the $M(CO)_{n-1}$ fragment.

We start with a single CO molecule at a very large distance from the rest of the system (step 0), which provides our reference orbitals and energy. In step 1, the CO molecule is put into its coordinated position with a frozen density. The molecular orbitals are in this step orthogonalized, which gives a repulsive contribution to the total energy which is rather different for the adsorbate and for CO in $Ni(CO)_4$. The initial repulsion is mainly due to the Pauli-repulsion and in particular due to the penetration of the CO 5σ-orbital, which has a large amplitude at the carbon atom, into the metal atom. The CO π-orbital on the other hand should not contribute to this initial repulsion in a significant way since π orbitals, as compared to σ, have a smaller spatial overlap with the Ni-orbitals. In addition, the 1π orbital on CO is mainly located on the oxygen as is also seen directly from the emission spectra.

In step 2, we keep the π orbitals frozen, which allows only for σ (and δ) type contributions to the total bond energy. In this step, polarization of the cluster and the adsorbate as well as possible covalent σ-type bond formation contribute to lower the energy. Finally, in step 3, also the π orbitals are allowed to relax and the final interaction energy is recovered.

By reversing the order of the σ and π relaxations, we find that the absolute values of the energy contributions from these can vary by about 0.2–0.3 eV, and we note that the total contributions of these steps are more or less equal in size, i.e.

Table 1
Constrained Space Orbital Variation Analysis for CO/Ni_{13}, $Ni(CO_4$ and $Cr(CO)_6$

Step	$Ni_{surf}+CO\rightarrow CO/Ni^{a}_{surf}$	$Ni(CO)_3+CO\rightarrow Ni(CO)^{b}_4$	$Cr(CO)_5+CO\rightarrow Cr(CO)^{c}_6$	$Cr+6CO\rightarrow Cr(CO)_6$	$Ni+4CO\rightarrow Ni(CO)_4$	$Cr(CO)_6$ Ziegler	$Ni(CO)_4$ Ziegler
0 (inf)	0 (1.146)	0 (1.146)	0 (1.146)	+0.88	+1.21	0	0
1 (frozen)	+4.73 (1.144)	+1.88 (1.142)	+1.33 (1.143)	+2.05	+4.36	+2.00	+1.85
2 (σ rel.)	+1.71 (1.139)	+0.44 (1.140)	+0.03 (1.135)			+0.31	+0.34
3(fully rel.)	−1.66 (1.175)	−1.57 (1.158)	−1.87 (1.161)			−1.52	−1.10

The interaction between the CO molecule and the remaining fragment is divided into initial repulsion, and separate σ and π-contributions. The definitions of steps 0–3 are given in the text. In the last two columns, we also tabulate values from calculations by Ziegler et al. [22], where a similar scheme was used to partition the interaction energy. The energies are reported in eV. The computed C–O bond lengths in Å associated with each step are given in parentheses. Metal–carbon distances: a, 1.75; b, 1.82; c, 1.91 Å.

σ and π relaxation are of equal importance. The stabilization we achieve in these steps includes both minimization of the repulsion and bond formation effects, which can only be distinguished by monitoring the accompanying orbital polarizations. In this respect the polarization of the CO σ system away from the metal, as well as σ-charge density loss for both CO and the metal (below), indicates that the repulsion dominates, while the π system is dominated by the bond formation.

We can directly note the difference between $Ni(CO)_4$ and adsorbed CO on Ni especially in the initial repulsion term. The main difference between the two systems is that the 4s orbital of Ni is to a large extent polarized away in the $Ni(CO)_3$ fragment, while on the Ni cluster the 4s electron is present. The larger σ polarization effects for CO/Ni_{13} as compared to $Ni(CO)_4$ seen in the calculated XE spectra in Fig. 2 are seemingly also reflected in the energetics.

Another way to perform an estimate of the energy cost related to the σ repulsion for $Cr(CO)_6$ is to start from the ground state of the Cr atom (septet) and keep the orbitals frozen as we place the six CO molecules in their positions (column 4). If we do it this way, we get a total initial repulsion of 29.41 eV, i.e. 4.90 eV per CO molecule, which is a large number, very close to the value obtained for CO on the Ni surface (4.73 eV). We could view this in another way, similar to the concept of bond preparation [23]. In order for the bond to form, the central metal atom must be prepared for bonding, which means an excitation from the ground state to a state where the CO molecules can penetrate to form the bond. This excitation cost from the septet to the desired singlet is for the case of $Cr(CO)_6$ 5.25 eV (0.88 eV per CO molecule). For this singlet the initial repulsion is 7.05 eV (1.17 eV per CO molecule), which is clearly lower than the almost 30 eV obtained for the septet.

In the case of $Ni(CO)_4$ (column 5) we find somewhat larger values, the excitation cost from the ground state to the bond-prepared state is 7.29 eV (1.21 eV per CO). The initial repulsion term is also larger, 12.60 eV (3.15 eV per CO).

It can be of interest to study how the density changes upon bond-formation of the CO to the substrate. Density differences have earlier been applied to investigate CO bonding by e.g. Wimmer et al. for CO/Ni(001) [24] and by Eichler and Hafner for CO/Pd(100) [25]. In both studies significant charge transfer was found, supporting a donation-back donation picture. In the present case we will refine this analysis by showing the charge density differences for CO/Ni_{13}, $Ni(CO)_4$ and $Cr(CO)_6$ for the σ- and π-symmetries separately (Fig. 5). If we start by considering CO/Ni_{13} (left panels) we find that there is an overall loss of charge in the σ- and a gain in the π- system. The fact that both the coordinated metal atom and CO loose charge in the σ-system is another clear indication of repulsive interaction, which is relieved through charge rearrangements. It is clear that on the metal this corresponds to a rehybridization from d_σ to d_π which can be expected to reduce the repulsion with the 5σ CO lone-pair. In the π-system we see both the formation of a carbon-nickel bond and the development of the lone-pair feature on the oxygen side. In the past [24] this has been interpreted as a population of a 2π* supporting a simple backdonation picture. However, from a detailed analysis of the orbitals we can identify 22% more population of 2π* and 12% depopulation of 1π upon coordination to the metal. The net effect is an increase in π population by 10%. The overall picture is thus a rehybridization of both the substrate Ni atom and the CO to reduce the repulsion and enhance the formation of the metal–adsorbate bond.

In this figure we also see the similarities between the CO adsorbed on the cluster representing the metal surface and the organometallic complexes in the middle and to the right. It seems that there in general is a loss of charge in the σ- and a gain of charge in the π-channels both on the metal and on the carbonyl. This can be viewed as a preparation for bonding through an excitation from σ-orbitals of the central metal atom into π-orbitals.

In Table 1 we also present how the calculated bond lengths are affected during the CSOV steps. In step 2 (σ interaction) the C–O bond length is shortened as compared to the frozen value, while in step 3, where also π interaction is taken into account, the bond lengths increase. A shortened bond length, as was the case in step 2, indicates an increased internal C–O bond strength. In order to understand this, we only need to consider the character of the interacting CO molecular orbitals. From calculations of molecular orbital overlap populations (MOOP) and frequency and bond-length shifts upon ionization of the σ orbitals of gas-phase CO, we find that the CO 3σ, 4σ and 5σ orbitals have strongly bonding, weakly bonding and weakly antibonding character, respectively. Indeed, the experimental bond distance of CO^+ ($X\ ^2\Sigma$) after ionization from the 5σ

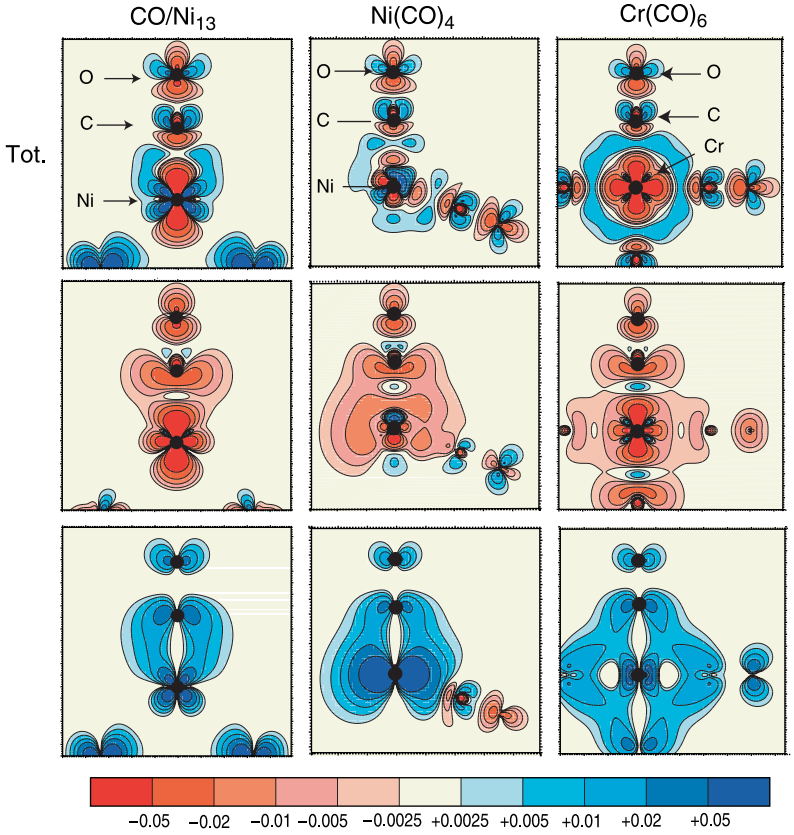

Fig. 5. Charge density differences, $\rho(CONi_{13})-\rho(CO)-\rho(Ni_{13})$ to the left, $\rho(Ni(CO)_4)-\rho(Ni)-\rho((CO)_4)$ middle, and $\rho(Cr(CO)_6)-\rho(Cr)-\rho((CO)_6)$ to the right. We plot the contributions from the total density (top), σ contribution (middle) and π contribution (bottom). Regions of electron loss are indicated in red (dashed outer line) and increase in blue (full line). We have chosen a plane containing the interacting metal atom with one CO along the z-axis in the plane in all three cases.

orbital is found to be shorter by 0.013 Å than for the neutral ground state [26]. This characterization of the orbital bonding characters is furthermore in agreement with previous theoretical work [27].

The antibonding character of the 5σ has also been proposed to explain the calculated bond length shortenings for HCO^+ and QCO^+, where Q is a point charge [28], for which no covalent π interactions are possible. For COH^+ and COQ^+ [28] however, a bond lengthening was found and it was concluded that the bond length shortenings probably are due to electrostatic effects rather than to σ interactions. However, this is actually a well-known trend for polar molecules [29]: transfer of charge from the more negative to the more positive species reduces the ionic character of the bond and enhances the covalent binding leading to a larger force constant since the latter depends on the overlap between orbitals. The reverse is true, as also found in references [28], when the polarizing field is reversed.

From investigations of the correlation between the vibrational frequency and the σ donation and π backdonation, it has been shown that frequency shifts correlate better with the amount of π backdonation than with the amount of σ donation [30]. This is expected, since the bond length change for 5σ ionization (here calculated to be −0.015 Å as compared to the experimental −0.013 Å [26]) is much smaller than the case of 1π ionization (+0.12 Å) or for the uptake of an electron in the 2π * orbital (+0.10 Å).

The reason why 5σ is antibonding is the large C(2s) character of this orbital which is in an antibonding phase with respect to the O(2pσ). Upon adsorption on the metal, a small part of the C(2s) character is lost which will strengthen the internal C–O bond. The π interaction on the other hand weakens the internal C–O bond, as indicated by the increased C-O distance. This is the case because the 1π and the 2π* hybridize, which gives an increased 2π* as well as a decreased 1π character in the occupied space. Both the occupation of 2π* and the decrease of 1π character will lead to a weakening of the internal bond. We can see that there is a compensation effect between the σ- and π-interactions both for the energetics and for the internal C–O bond strength. Again we can see a similar behavior for CO adsorbed and coordinated to Ni.

Let us now look at the other metal carbonyls, $Fe(CO)_5$ and $Cr(CO)_6$, and see how the orbital structures in these are consistent with our observations for $Ni(CO)_4$. In Fig. 2 we can see that the π spectra are very similar. We again demonstrate the allylic configuration in $Fe(CO)_5$ by displaying some of the π-orbitals extending over the whole metal carbonyl molecule as shown in Fig. 6. There is a class of symmetrized molecular orbitals that represents the local $1\tilde{\pi}$, $\tilde{d}_\pi$ and $2\tilde{\pi}^*$ type interactions. However, the π electronic structure is very similar for all the metal carbonyls.

If we instead look at the σ electronic structure represented by the computed XES spectra in Fig. 2 we can see a splitting of

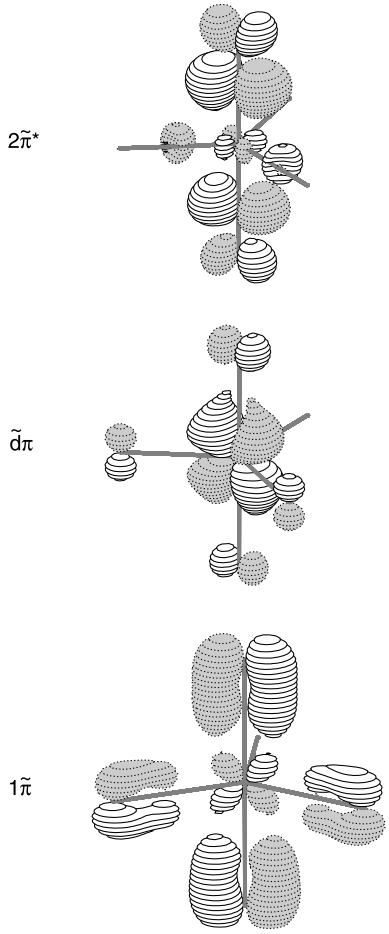

Fig. 6. π orbitals of $Fe(CO)_5$.

the 4σ and the 5σ levels into several features. This is due to the generation of symmetry orbitals in the appropriate point group. There is even a different polarization between carbon and oxygen for the different orbitals. However, the overall picture is the same with a polarization of the $5\tilde{\sigma}$ orbital towards oxygen and of the $4\tilde{\sigma}$ towards carbon (mainly C(2s) character).

As a last example of the allylic formation in the π orbitals, we display in Fig. 2 the computed XES spectra and in Fig. 7 some representative π orbitals for CO attached to the iron atom of the heme group in hemoglobin. Not unexpectedly, we find the same features as for all the other cases, with an increased carbon character of the $1\tilde{\pi}$ feature as compared to gas-phase and also the typical oxygen lone-pair feature. Interestingly, we find a clear separation of the $\tilde{d}_{\pi}$-b and $\tilde{d}_{\pi}$-t orbitals, which is driven by the porphyrin ligand, which clearly can be seen as an important contribution in the $\tilde{d}_{\pi}$-b orbital seen in Fig. 7. The $\tilde{d}_{\pi}$-t orbital being the HOMO has an equal amount of oxygen and carbon character which is a sign of increasing 2π* character. The σ system again shows the typical polarization of 5σ towards the oxygen, and an increasing C(2s) character of 4σ.

Thus we can conclude that the allylic formation of the π orbitals and also the strong polarization of the σ system seem to be a general aspect of the interaction between carbonyls and

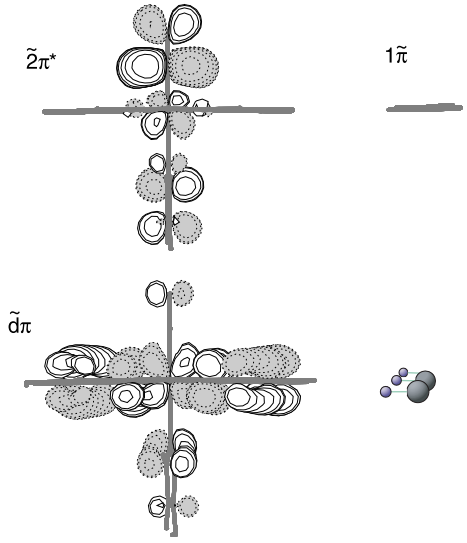

Fig. 7. Three π orbitals for CO on hemoglobin.

metals. However, there are some important differences in the total bond energies. If we compare the energetics for $Cr(CO)_6$ with $Ni(CO)_4$ in Table 1 we find a somewhat lower initial repulsion (step 1) in the case of $Cr(CO)_6$.

The initial repulsion is very much dependent on the C-metal distance, which is shorter in the case of $Ni(CO)_4$ (1.82 Å) compared to $Cr(CO)_6$ (1.91 Å). The most important difference in the electron configuration of $Ni(CO)_4$ and $Cr(CO)_6$ was found to be a larger d_{σ} occupation for $Ni(CO)_4$. This should make the repulsion term larger for Ni. After the relaxation of the σ system $Cr(CO)_6$ is almost net bonding, whereas $Ni(CO)_4$ is still repulsive by 0.44 eV. The difference seems related to the initial repulsion. The σ-system can be described using a simplified MO diagram with the metal-bonding $5\tilde{\sigma}$ and $4\tilde{\sigma}$ orbitals and antibonding $\tilde{d}_{\sigma}$ orbitals. We can directly see in Fig. 2 that the antibonding $\tilde{d}_{\sigma}$ orbital is occupied in $Ni(CO)_4$ and unoccupied in $Cr(CO)_6$. Population of antibonding orbitals leads to Pauli repulsion in the case of $Ni(CO)_4$ whereas in $Cr(CO)_6$ the σ system is more weakly interacting with a resulting low repulsion.

We do not make any attempt to completely summarize the abundant literature with different results for all carbonyl complexes, instead we refer to e.g. Ref. [1] for a more complete review of the area. For the purpose of the present discussion we will focus on a comparison with previous studies where similar divisions of the different contributions to the bond energetics have been made. In a study by Ziegler *et al.* [22] the bonding in several metalorganic complexes, e.g. $Cr(CO)_6$ and $Ni(CO)_4$ was studied using DFT without gradient corrections. Also here a partitioning of the bond energy contributions similar to the CSOV scheme was used. The interacting fragments were taken as either the $(CO)_n$ and the bare metal atom or as MCO_{n-1} and CO, where the latter case is similar to our approach and is included for comparison in Table 1. We find that the energetical values are somewhat different as compared to our calculated values due to the different functionals used. The overall picture is, however, very much the same in both

investigations with a net repulsion before allowing for π interactions, which we interpret as the σ repulsion.

In another DFT study by Davidson *et al.* [31,32], the bond of $Cr(CO)_6$ was described in terms of an energy decomposition analysis (EDA) partitioning scheme which is similar to the CSOV scheme presented in the present paper. In that study, the starting point was a free Cr atom and a free $(CO)_6$ cluster. The first step was the excitation of the Cr atom from the ground state d[5]s[1] to the hypothetical excited d[6]s[0] configuration. This excitation decreases the initial repulsion when the two fragments are brought together, since the repulsion towards 4s is removed. The initial repulsion and the excitation constituted a total energy cost of 1.87 eV per CO molecule. The partitioning into σ and π contributions was only done at the Hartree–Fock level, but suggested that the π contributions are larger than that due to σ. A comparison to our results is not perfectly adequate, since we use different interacting fragments, but also here the picture of a net σ repulsion and π bonding seems valid.

Interesting to note is that in the work by Davidson et al. the contour plot of the $\tilde{d}_\pi$ orbital is shown. The authors, as well as the authors of Ref. [1], note that this orbital has very little metal–CO bonding character and therefore attribute the main part of the bonding as due to a relaxation of the 3d electrons rather than a covalency effect. However, as shown in the present work, the bonding is provided by the $1\,\tilde{\pi}$ orbital and the non-bonding $\tilde{d}_\pi$ is just a natural consequence of the orbital mixings within the allylic three-level bonding scheme.

Previous studies, e.g. [22,33] on surfaces and carbonyl complexes agree that the π* 'backdonation' is more important than the σ 'donation' for the metal-CO bond energy. In the σ system, stabilization effects due to the penetration of the 5σ orbital into the metal atom to form an electrostatic interaction between 5σ and the metal nucleus have also been discussed, see e.g. ref. [31,34]. This type of bonding requires first a polarization of charge away from the metal atom in order for the attraction between the 5σ and the nucleus to be significant.

The amount of σ repulsion will depend on the number of occupied σ-orbitals on the metal and thus a smaller repulsion is expected for metals to the left in the transition row. In Fig. 8 we compare the computed XES spectra for gas phase TiCO ($^5\Delta$) and NiCO ($^1\Sigma^+$) and relate them to the relative positions of the levels involved in the interaction. The 3d orbitals become more destabilized as one moves from the right to the left in the transition row; for Ti the 3d-level is found near-degenerate with the CO π* while for Ni this level is in a position more intermediate between the two CO levels.

This affects the amount of mixing between the orbitals in the three-level interaction as is also expected from a perturbation theory approach. Thus, the lone-pair state, discussed above as one of the components in the allylic configuration, is not a pure non-bonding orbital in either of these cases, but still retains some carbon character. The interaction in the π symmetry is stronger, per interacting spin-orbital, for the TiCO as seen from the higher total CO intensity in the non-bonding orbital than for the NiCO (note that the carbon and oxygen contributions are equal in the TiCO case). From the relative intensities of the

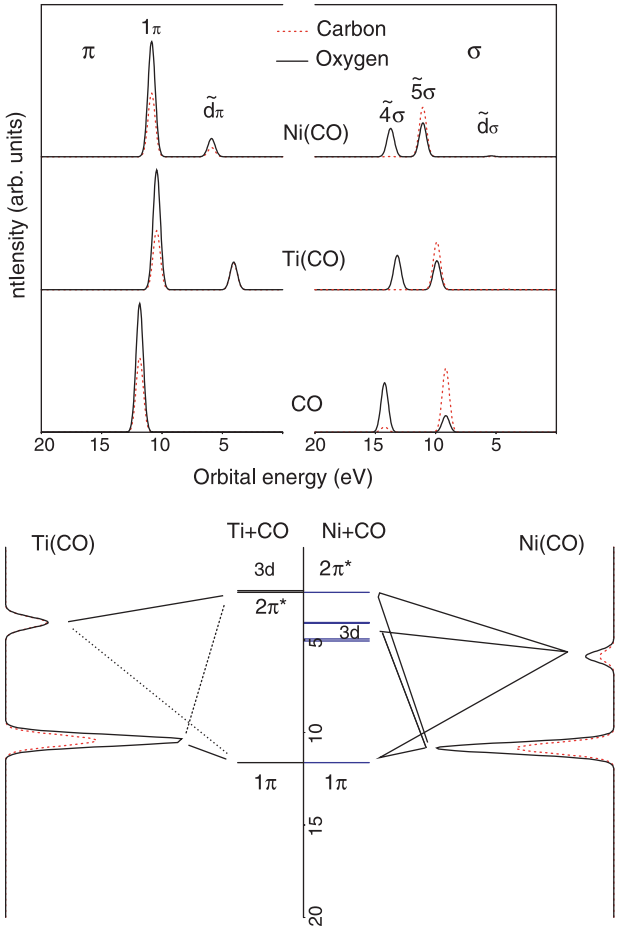

Fig. 8. Computed XE spectra for gas phase TiCO ($^5\Delta$) and NiCO ($^1\Sigma^+$) in comparison with gas phase CO. The resulting orbital interaction diagram for the π-system is given in the lower part of the figure, where the dotted lines indicate a smaller admixture. Note that the essentially non-bonding orbital in TiCO contains equal contributions from carbon and oxygen.

carbon and the oxygen contributions we can say that the amount of π* involvement is greater in TiCO than in NiCO; this is also seen from the larger increase in the $1\tilde{\pi}$ and reduction of the $2\tilde{\pi}$ orbital energies relative to gas phase CO for TiCO than NiCO. That a bonding orbital actually increases in orbital energy upon bond formation may seem counterintuitive, but is a result of the need to also internally hybridize with the higher-lying π* in order to form the bond.

For the σ symmetry we find that the TiCO orbitals are somewhat less perturbed by the repulsion than the NiCO; the energy gained in a CSOV analysis in relaxing the σ symmetry completely from the initial frozen gas phase orbitals is indeed of the order of 1 eV for TiCO and 2.4 eV for NiCO. All in all this represents further confirmation of the orbital rotation picture where all levels are perturbed and mixed to an extent that depends on the interaction strength and the energy matching of the levels involved.

We can conclude that our picture of chemical bonding of CO to metal surfaces and in carbonyls is in agreement with results from many previous studies. The picture in the present work is based on experimental measurements of the molecular orbitals in combination with calculations. It turns out to be

essential to consider important redistributions of the atomic contributions to all molecular orbitals upon interaction with the metal. This MO picture together with an energetic subdivision of the different contributions has provided a refined model of the CO–metal interaction in terms of an allylic π bonding configuration and a σ repulsive interaction. The amount of σ repulsion depends strongly on the electronic configuration of the metal, and in special cases it can be small enough that the σ donation picture is appropriate.

4. Conclusions and summary

We have examined how CO binds to metals in a number of examples from surface physics and metal-organic chemistry through the use of X-ray emission spectroscopy and calculations. The unique experimental setup made it possible to probe the electronic structure of N_2 and CO on metal surfaces in an atom- and symmetry-specific manner. Comparison to theoretical calculations shows that an orbital description of these systems is to a large extent valid. A simple frontier orbital description involving only the 5σ and the $2\pi^*$ orbitals on the CO molecule is shown not to describe the electronic structure of these systems correctly. Instead, we find large changes in all orbitals of the σ- and the π systems. The electronic structure changes in the π orbitals are better described in terms of the formation of an allylic configuration involving the CO 1π, $2\pi^*$ and the Ni $3d_\pi$ orbitals where the amount of mixing depends on the interaction strength and the energy matching of the d-levels with those of the CO. In the σ system, all CO and Me orbital interactions occur in the occupied space resulting in Pauli repulsion. This is minimized by polarization of charge away from the CO–Me bond. In the present work this picture is shown to be valid also for a number of different organometallic complexes, from which it is clear that this orbital interaction scheme is general. The description of the bond formation refines the normal Dewar–Chatt–Duncanson model, which predicts σ donation and π backdonation, to involve σ repulsion and π bonding. Although this picture has been proposed previously based on theoretical work, this bonding picture is now also supported by direct measurements of the molecular orbitals for surface adsorbed CO and N_2.

We thank the staff at the ALS for all their assistance. This research was sponsored by the Swedish Natural Science Research Council (NFR) and by the Göran Gustafssons Foundation for research in natural science and medicine.

References

[1] G. Frenking, N. Fröhlich, Chem. Rev. 100 (2000) 717.
[2] D. Michael, P. Mingos, J. Organomet. Chem. 635 (2001) 1.
[3] M.J.S. Dewar, Bull. Soc. Chim. Fr. 18 (1951) C79.
[4] J. Chatt, L.A. Duncanson, J. Chem. Phys. (1953) 2939.
[5] G. Blyholder, J. Phys. Chem. 68 (1964) 2772.
[6] A. Nilsson, M. Weinelt, T. Wiell, P. Bennich, O. Karis, N. Wassdahl, J. Stöhr, M.G. Samant, Phys. Rev. Lett. 78 (1997) 2847.
[7] P. Bennich, T. Wiell, O. Karis, M. Weinelt, N. Wassdahl, A. Nilsson, M. Nyberg, L.G.M. Pettersson, J. Stöhr, M.G. Samant, Phys. Rev. B 57 (1998) 9274.
[8] A. Föhlisch, M. Nyberg, P. Bennich, L. Triguero, J. Hasselström, O. Karis, L.G.M. Pettersson, A. Nilsson, J. Chem. Phys. 112 (2000) 1946.
[9] A. Föhlisch, M. Nyberg, J. Hasselström, O. Karis, L.G.M. Pettersson, A. Nilsson, Phys. Rev. Lett. 85 (2000) 3309.
[10] A. Nilsson, L.G.M. Pettersson, Surf. Sci. Rep. 55 (2004) 49.
[11] A. Föhlisch, N. Wassdahl, J. Hasselström, O. Karis, D. Menzel, N. Mårtensson, A. Nilsson, Phys. Rev. Lett. 81 (8) (1998) 1730.
[12] A. Nilsson, M. Weinelt, T. Wiell, P. Bennich, O. Karis, N. Wassdahl, J. Stöhr, M.G. Samant, Phys. Rev. Lett. 78 (1997) 2847.
[13] M. Nyberg, J. Hasselström, O. Karis, N. Wassdahl, M. Weinelt, A. Nilsson, L.G.M. Pettersson, J. Chem. Phys. 112 (2000) 5420.
[14] T.A. Albright, J.K. Burdett, M.H. Whenghbo, Orbital Interactions in Chemistry, Wiley, New York, 1985.
[15] Principal authors: M.E. Casida, C. Daul, A. Goursot, K. Hermann, A. Koester, L.G.M. Pettersson, E. Proynov, A. St-Amant, and D.R. Salahub. Contributing authors: V. Carravetta, H. Duarte, N. Godbout, J. Guan, C. Jamorski, M. Leboeuf, V. Malkin, O. Malkina, M. Nyberg, L. Pedocchi, F. Sim, L. Triguero, A. Vela, deMon-KS StoBe version 1.0, deMon Software, 2001.
[16] J.P. Perdew, Y. Wang, Phys. Rev. B, 45 (1992) 13244; J.P. Perdew, in: P. Ziesche, H. Eischrig (Eds.), Electronic Structure of Solids, Akademie Verlag, Berlin, 1991; J.P. Perdew, J.A. Chevary, S.H. Vosko, K.A. Jackson, M.R. Pederson, D.J. Singh, C. Fiolhais, Phys. Rev. B, 46 (1992) 6671.
[17] L. Triguero, L.G.M. Pettersson, H. Ågren, Phys. Rev. B 58 (1998) 8097; L. Triguero, L.G.M. Pettersson, H. Ågren, J. Phys. Chem. A 102 (1998) 10599.
[18] A. Föhlisch, J. Hasselström, P. Bennich, N. Wassdahl, O. Karis, A. Nilsson, L. Triguero, M. Nyberg, L.G.M. Pettersson, Phys. Rev. B 61 (2000) 16229.
[19] A. Nilsson, J. Hasselström, A. Föhlisch, O. Karis, L.G.M. Pettersson, M. Nyberg, L. Triguero, J. Electron Spectrosc. Relat. Phenom. 110–111 (2000) 15.
[20] P.S. Bagus, K. Hermann, C.W. Bauschlicher, J. Chem. Phys. 80 (1984) 4378; P.S. Bagus, K. Hermann, C.W. Bauschlicher, J. Chem. Phys. 81 (1984) 1966.
[21] I. Grinberg, Y. Yourdshahyan, A.M. Rappe, J. Chem. Phys. 117 (2002) 2264.
[22] T. Ziegler, V. Tschinke, C. Ursenbach, J. Am. Chem. Soc. 109 (1987) 4825.
[23] I. Panas, J. Schüle, P. Siegbahn, U. Wahlgren, Chem. Phys. Lett. 149 (1988) 265.
[24] E. Wimmer, C. Fu, A. Freeman, Phys. Rev. Lett. 55 (1985) 2618.
[25] A. Eichler, J. Hafner, Phys. Rev. B 57 (1998) 10110.
[26] K.P. Huber, G. Herzberg, Molecular Spectra and Molecular Structure, Van Nostrand Reinhold, New York, 1979.
[27] W.A.G. Graham, Inorg. Chem. 7 (1968) 315; R.L. DeKock, A.C. Sarapu, R.F. Fenske, Inorg. Chem. 10 (1971) 38; M.B. Hall, R.F. Fenske, Inorg. Chem. 11 (1972) 768; A.W. Ehlers, E.J. Baerends, F.M. Bickelhaupt, U. Radius, Chem. Eur. J. 4 (1998) 210; U. Radius, F.M. Bickelhaupt, A.W. Ehlers, N. Goldberg, R. Hoffmann, Inorg. Chem. 37 (1998) 1080.
[28] A.J. Lupinetti, S. Fay, G. Frenking, S.H. Strauss, J. Phys. Chem. 101 (1997) 9551; A.S. Goldman, K. Krogh-Jespersen, J. Am. Chem. Soc. 118 (1996) 12159.
[29] V. Gutmann, The Donor–Acceptor Approach to Molecular Interactions, Plenum Press, New York, 1978; V. Gutmann, Pure Appl. Chem., 512197; W.J. Mortier, J. Sauer, J.A. Lercher, H. Noller, J. Phys. Chem., 88905.
[30] A.W. Ehlers, S. Dapprich, S.F. Vyboischikov, G. Frenking, Organometallics 15 (1996) 105.
[31] E.R. Davidson, K.L. Kunze, F.B.C. Machado, S.J. Chakravorty, Acc. Chem. Res. 26 (1993) 628.
[32] K.L. Kunze, E.R. Davidson, J. Phys. Chem. 96 (1992) 2129.
[33] C.W. Bauschlicher, P.S. Bagus, J. Chem. Phys. 81 (1984) 5889; L.A. Barnes, M. Rosi, C.W. Bauschlicher, J. Chem. Phys. 94 (1991) 2031.
[34] P.S. Bagus, K. Hermann, Phys. Rev. B 33 (1986) 2987; C.R. Brundle, P.S. Bagus, D. Menzel, K. Hermann, Phys. Rev. B 24 (1981) 7041; P.S. Bagus, C.J. Nelin, C.W. Bauschlicher, Phys. Rev. B 28 (1983) 5423; P.S. Bagus, K. Hermann, C.W. Bauschlicher, Phys. Rev. B 30 (1984) 4378; K. Hermann, P.S. Bagus, C.J. Nelin, Phys. Rev. B 35 (1987) 9467.